Article

JFPE

Journal of Fire Protection Engineering
22(3) 197–225

DOI: 10.1177/1042391512448303
jfe.sagepub.com

SAGE

Fire growth simulation in passenger rail vehicles using a simplified flame spread model for integration with CFD analysis

Kurt Schebel
Arup USA, New York, NY, USA

Brian J Meacham
Worcester Polytechnic Institute, Worcester, MA, USA

Nicholas A Dembsey
Worcester Polytechnic Institute, Worcester, MA, USA

Matthew Johann
Arup USA, Cambridge, MA, USA

Jeffrey Tubbs
Arup USA, Cambridge, MA, USA

Jarrod Alston
Arup USA, Cambridge, MA, USA

Abstract

Few robust engineering approaches currently exist to assess flame spread performance of interior finish materials for a range of source fires, in support of compartment fire hazard analysis. As a step toward closing this gap, a simplified approach for assessing (a) the propensity for a material to support self-propagating flame spread and (b) the extent of flame spread for a range of source fire conditions has been developed. In addition, a general approach for integrating the output of the simplified flame spread

Corresponding author:
Kurt Schebel, Arup USA, 77 Water St., New York, NY 10005, USA
Email: Kurt.Schebel@Arup.com

analysis into a computational fluid dynamics (CFD) model has been developed to predict the overall fire growth and spread hazard for a passenger rail vehicle compartment.

Keywords
Flame spread model, b-parameter, compartment fires, design fires, computational fluid dynamics, fire dynamics simulator, passenger rail vehicles

Introduction

Fire development in a passenger rail vehicle will be influenced by the size and location of the source fire, the type, amount and characteristics of fuel available to burn (e.g. interior linings, seating materials and contents), vehicle configurations, and other passenger-related items that may be carried onboard. Any given combination of these parameters can significantly affect the ultimate fire size. Factors such as the effects of adjacent materials on fire spread and growth, the potential for flame spread away from the fire origin, and ventilation conditions must also be considered. For instance, a fire initiating on the floor adjacent to a stainless steel panel and away from any seats will not likely grow to a significant size because of the absence of fuel. However, a fire on a seat directly adjacent to a clear plastic advertisement panel that extends upward to a plastic laminate ceiling panel may result in significant flame spread and a large ultimate fire size.

Although computational analysis is commonly used to help simulate fires in passenger rail vehicles, the typical focus is to assess vehicles in tunnels having associated ventilation requirements [1–3]; the initial stages of the fire development in such environments are often not considered. In part, this approach is driven by past vehicle fires in tunnels and a desire to understand the potential severe case fires for ventilation needs [2]. However, if the vehicle fire hazard assessment is based solely on past rail and tunnel fire experience and does not consider the specific characteristics of the vehicle in question, opportunities to reduce the maximum heat release rate (HRR) of the vehicle by reducing the overall contribution of the vehicle materials or through other options might be missed. In addition, from a risk and security management perspective, such approaches may not provide sufficient means to help assess the potential for source fires of various sizes to lead to full vehicle involvement. For these analyses, a better understanding of the propensity for interior materials to support flame spread, and the ability to better incorporate flame spread into the computational analysis, is needed. Although this need has been recognized [2,4], little has been published regarding tools and approaches to address the initial stages of fire spread and development in passenger rail vehicles.

As a step toward better understanding of the relationship between source fire conditions (size, location), properties of interior lining materials (e.g. walls and ceilings), and the propensity for growth to full-vehicle involvement, research has

been conducted that considers these factors [5]. Key outcomes of this research include (a) development of a 'go/no-go' screening approach for assessing the propensity of interior lining materials to facilitate self-propagating flame spread using material property data from a laboratory apparatus, (b) development of a simple formula-based engineering tool to assess initial flame spread, and (c) development of a method to incorporate the flame spread characteristics into a computational fluid dynamics (CFD) model. In this study, the laboratory apparatus is the cone calorimeter [6], which is a readily available and economical test methodology that supports consideration of a wide range of heat fluxes, while the CFD model is fire dynamics simulator (FDS) [7]. The screening tool results in the calculation of a value referred to here as the 'b-parameter', which is indicative of a given material's propensity to spread flame or self-extinguish.

While a similar approach is described in work aimed at validating FDS against bench-scale (single burning item) and full-scale tests using cone calorimeter data [8], the approach outlined here provides a process for engineers to follow in the hazard assessment of existing vehicles and for material selection in new vehicles. The current analysis demonstrates the utility of using the b-parameter [9,10] and simplified upward flame spread modeling for initial screening, and indicates how burner surfaces can be utilized within FDS to simulate the concept of flame spread in a compartment. This approach is applied following the steps outlined below and shown in Figure 1.

1. Identify vehicle configuration parameters that contribute to fire growth. This should include specific vehicle interior arrangements (seating, partitions, etc.), interior materials, and sources of potential ignition.

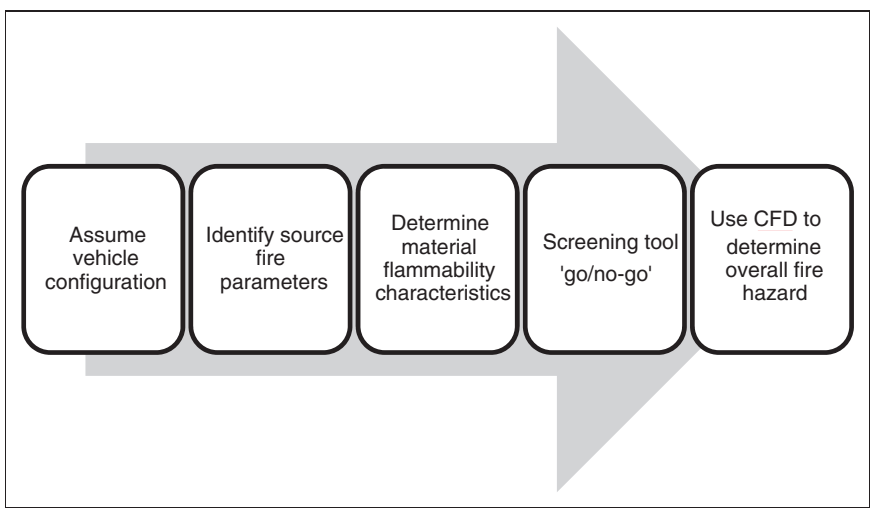

Figure 1. Fire spread assessment approach.

2. Characterize the source fires of concern in terms of heat flux exposure to target of concern (e.g. wall, ceiling, etc.). This will include consideration of the types, amounts and locations of materials that may burn.
3. Determine material flammability characteristics of interior lining materials through cone calorimeter testing. Expose materials to a range of heat fluxes as discussed in the 'Material flammability characteristics' section.
4. Determine the b-parameter for each material. Assess 'go/no-go' status of flame spread given material properties and source fire scenarios of concern. If the high level 'go/no-go' analysis is insufficient for hazard assessment needs, estimate flame spread behavior through formula-based flame-spread analysis. If final conclusions regarding the fire hazard of the proposed materials can be derived based on the calculated b-parameters and this simplified flame spread modeling, and there are not other fire hazard concerns (such as unique geometrical arrangements or ventilation factors often found in the complexity of passenger trains), analysis is complete. If not, continue to Step 5 below.
5. Determine CFD model input parameters needed to simulate various fire scenarios within the vehicle. Model initial flame spread as a series of burners that together recreate the flame spread behavior predicted by the formula-based analysis in Step 3 above. Model adjacent surface materials through application of a genetic algorithm (GA) analysis using the cone calorimeter data. The GA analysis determines optimized material properties through an automated process that considers tens of thousands of trial solutions. Details of this process can be found in the literature [19]. Use CFD results to inform the material choice and to help understand the overall fire hazard associated with the vehicle. Details for this approach can be found in the 'integration with CFD' section.

Illustrative example

The application of the analytical approach outlined above will be demonstrated in the remaining part of this article through a practical example aimed at showing how one can assess the relative fire hazard associated with interior lining materials in a passenger rail vehicle. It should be noted that the example reflects materials that are commonly used in passenger rail vehicles and typical vehicle design parameters. Its purpose is to demonstrate the analysis methodology that has been proposed, and is not intended as a source for input data to support fire modeling or analysis [5,11].

The present section defines the basic premise of the illustrative example; subsequent sections will refer to this example in order to demonstrate the concepts being discussed.

For this example, assume an urban rail operator is adding a series of new vehicles to their system. Tunnel and station fire and life safety features (suppression, smoke exhaust, etc.) are not being upgraded, so the new vehicles must be designed with attention to the constraints of the existing fire and life safety systems. In particular, smoke control systems are sized to address fire scenarios with maximum total HRRs no larger than 11 MW, and these systems cannot be upgraded.

The rail vehicle design team has narrowed the choice of interior wall and ceiling linings to two glass-reinforced polymer (GRP) material options. Full-scale fire tests of these materials in the vehicle installation are not possible within the design budget or schedule. The materials being considered are labeled GRP A and GRP B for the purposes of this analysis.

Identify fire scenarios

As revealed from assessing past events [4,5], a wide range of fire scenarios may be anticipated in passenger rail vehicles. To help determine the scenarios of concern, a fire threat, vulnerability, consequence and risk assessment (TVCRA) may be warranted [12]. A fire TVCRA would consider sources of potential ignition, initial fuels and resulting initiation fires (threats), the potential for propagating the initiation fire within the vehicle (vulnerability), the impact of the growing/developed fire (consequence), and where desired, an assessment of the probability of event occurrence (risk). For the purpose of this article, the focus is limited to assessing the potential of an initiation fire to ignite interior finish materials, the ability of those materials to propagate flame spread once ignition occurs, and the contribution of the interior materials to the total HRR (vulnerability and consequence assessment).

Assuming that one has identified the fire threats of concern, one then needs to assess the potential for ignition of secondary fuels: in the context of this article, interior lining materials. In order to quantify whether an initiating fire is likely to ignite adjacent lining materials, the thermal exposure resulting from the initial fire needs to be considered. To evaluate whether a material will ignite under a given fire exposure, the material's critical heat flux (CHF) must be reviewed [13]. CHF is the minimum heat flux at or below which a material does not generate sufficient combustible vapors to support combustion. Quintiere [14] describes how these parameters and others can be derived from small-scale test data. Dembsey and Williamson [15] describe the value of estimating the critical ignition source strength for predicting flame spread potential.

Different combustible materials require different levels of incident heat flux in order to ignite. In some cases, the required heat fluxes may not be possible given credible design fires. It is important to review the likely fires within the vehicle being studied in order to understand the hazards they present to the lining materials.

As part of the fire TVCRA, the engineer will have to characterize the source fire(s) of concern, estimate the heat flux exposure to the target surface generated by the source fire(s), assess the potential for ignition of the secondary fuels, and assess the propensity for the fire to continue to develop and spread. Various approaches for estimating the heat flux to a target surface are readily available [14]. Although there are many items that might be considered, at the scale of interest for this approach, the source fire heat flux is expected to be the dominating factor. As such, key steps include estimation of the heat flux(es) at the target, the exposure time(s) at the estimated heat flux level(s), and the shape and area of the exposure.

For the example used here, the source fire consists of several bags of trash on the floor against a wall of the vehicle. Such a fuel load is representative of a mixture of combustible materials contained within a relatively small fixed volume, as may be typical of items carried on to a passenger rail vehicle. This is modeled as a fire HRR of approximately 500 kW which results in an incident heat flux to the wall of 50 kW/m^2 over a rectangular area of height 1 m and width 0.6 m; further discussion is provided in Appendix C. In this scenario, the wall is considered to be the initial material burning. Flame spread to additional surfaces (i.e. ceiling, floor and seats) is incorporated through the use of CFD analysis.

Material flammability characteristics

Once the source fire has been characterized, the next step is to determine whether the interior lining materials are vulnerable to flame propagation and fire development. Given a focus on flame spread, information is required regarding the properties of vehicle materials as outlined above. Such properties can be obtained from cone calorimeter [6] test data. These data are used as part of a first-order 'go/no-go' screening tool that involves evaluation of the b-parameter to help determine, if different vehicle lining materials are likely to support flame spread at various heat flux levels. For any representative heat flux, independent of initial conditions, if the b-parameter is greater than zero, the flame is predicted to accelerate and spread; but if the b-parameter is less than zero, the flame is predicted to decelerate and eventually extinguish itself. By assessing a material's b-parameter at various heat fluxes, a first-order assessment of flame spread potential under different source fire and compartment conditions can be obtained.

The b-parameter, as shown in equation (1), utilizes parameters measured or derived from cone calorimeter results. The theoretical basis of this equation can be found in the work of Cleary and Quintiere [9,10].

$$b = 0.01\dot{E}'' - 1 - \frac{t_{ig}}{t_{bo}} \tag{1}$$

Where, $\dot{E}''$ is the average HRR per unit area (kW/m^2), t_{ig} is the time to ignition in the cone calorimeter and t_{bo} is the measured burnout time. (For the purposes of this study, t_{end} is measured as the time to flame out, time when the HRRPUA < 50 kW/m^2, as further discussed below.)

A cone calorimeter [6] heat release rate per unit area (HRRPUA) graph for each tested incident heat flux is needed to develop the input for b-parameter calculation. Geometric instabilities, cellular flames and extended tail-like results can affect the analysis results. Cellular flames, which are physically observed and recorded during each cone calorimeter test, can represent unstable flames that flash during tests. Long tail-like results at the end of a cone test are due to non-uniform or edge burning that result in extended values and burning times. This tail-like behavior can lead to lower HRRPUA averages, if not identified and omitted. To account for

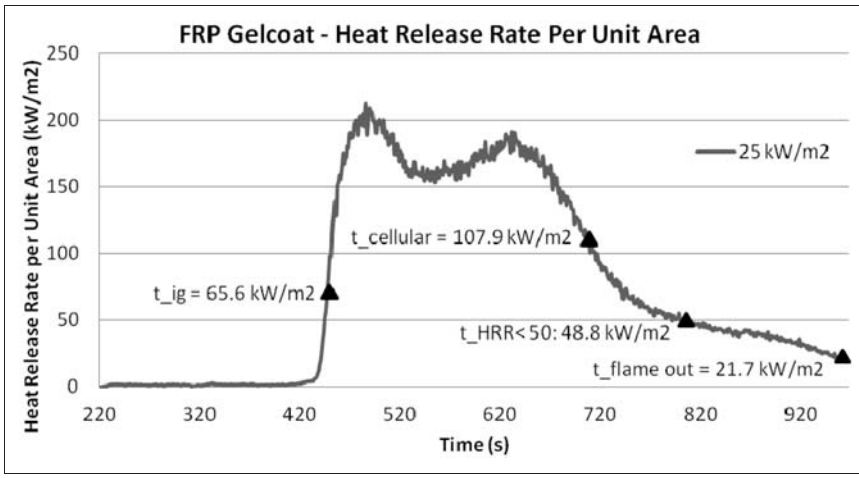

Figure 2. Representative material – 25 kW/m^2 cone calorimeter results.

these behaviors, each test is independently analyzed. Figure 2 shows derived cone calorimeter HRRPUA results for a representative FRP material at a heat flux of 25 kW/m^2. Average HRRPUA can be determined via integration from the observed ignition time to the time when the HRRPUA becomes less than 50 kW/m^2, as utilized in this analysis to reduce the effects of unstable flames.

Variations in the cone calorimeter setup, testing methodology and approaches for post-processing of data may influence results, and the engineer must consider these impacts and validate the approach used, as required.

After t_{ig}, t_{bo} and average HRRPUA are observed or derived from tests, the b-parameter value can be calculated from equation (1).

The b-parameter is used to compare GRP A and GRP B utilizing characteristics measured in the cone calorimeter [6]. In this instance, it is important to quantify the tendency of the material to spread flame at a range of heat fluxes likely seen from initiation fires observed in rail cars. Table 1 shows average HRRPUA values for GRP A and GRP B at cone incident heat fluxes of 15, 20, 50 and 75 kW/m^2 with the respective b-parameters. It can be seen that GRP B has positive b-parameter values for all heat flux levels, indicating that it has a tendency to spread flame. This is especially true given heat flux values in excess of 20 kW/m^2 for which strongly positive b-parameter values are calculated. The b-parameter calculated for a heat flux exposure of 15 kW/m^2 is not definitive, and thus would likely warrant further review. However, unlike GRP B, GRP A exhibits negative b-parameters given a heat flux of 20 kW/m^2 or less. Even at a heat flux level of 75 kW/m^2, the b-parameter calculated for GRP A is less than that calculated for GRP B given a much lower heat flux (20 kW/m^2).

Results such as those presented in Table 1 can be used as a screening tool in identifying likelihood of a material to spread flame in an acceleratory manner or simply to extinguish itself. Owing to the uncertainty in measurements and

Table 1. Calculated b-parameter values

Material	Heat flux (kW/m^2)	Average HRRPUA (kW/m^2)	b-parameter
GRP A	15	92.1	−0.60
	20	98.4	−0.28
	50	145	0.31
	75	158	0.50
GRP B	15	166	0.20
	20	206	0.64
	50	272	1.60
	75	236	1.33

GRP: glass-reinforced polymer; HRRPUA: heat release rate per unit area.

calculations, it is important to note that b-parameter values furthest from zero provide more definitive results [16], where maximum b-parameter uncertainty is estimated to be 0.7 full scale.

Appendix A provides b-parameter data sets for various materials found in passenger rail vehicles and further illustrates the usefulness of the screening tool.

Flame spread tool

If the b-parameter screening analysis indicates that a material has a propensity to propagate flame spread, additional vulnerability assessment is warranted. To support this, a simplified upward flame spread model based on the work of Mowrer and Williamson [17] was developed to represent the initial flame spread on vehicle lining materials. It should be noted that flame spread is a complex phenomenon, and certain bounding conditions and assumptions have been made in this simplified model. Notably, the model uses only parameters measured in small-scale tests (i.e. the cone calorimeter) and equations that model flame height, pyrolysis height and burnout height. Front velocities (e.g. the flame spread velocity) can also be developed from this model, and HRRs are calculated from the spread results to better understand the fire hazards.

Figure 3 illustrates characteristics of upward flame spread [17]. The overall flame height, x_f, results from the burning of the wall material. The pyrolysis height is represented by x_p. When the fuel is considered spent or used up, it can no longer support a flame and a burnout front develops, indicated by x_b.

The initial source fire imposes a heat flux on the wall, q''_e. If the heat flux is sufficient to ignite the wall material, the flame extends up the wall, in turn emitting a flame heat flux, q''_f to the virgin fuel above. For the purposes of this model, preheating caused by convection and radiation from the upper gas layer is ignored.

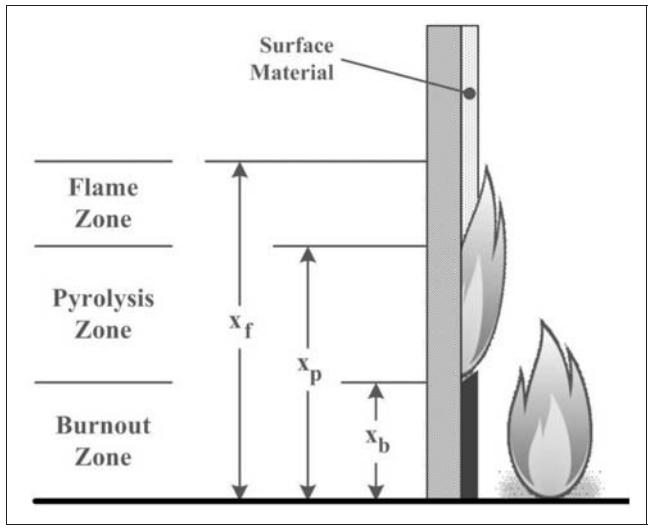

Figure 3. Upward flame spread model.

The idealized heat flux distribution reveals the potential heat fluxes involved, assuming that the flame heat flux up the wall is constant. For the purposes of this study, the incident heat flux used in the cone calorimeter [6] is also used as the external heat flux as well as flame heat flux. This is a reasonable approximation because the incident heat flux in the cone calorimeter is not significantly affected by the flames formed under the cone. See Appendix B for additional discussion relative to wall heat fluxes and cone calorimeter heat fluxes.

A model of the illustrative example was created to demonstrate how these parameters relate to one another and how they change over time. It is important to note that flame spread along the wall is concurrent flow flame spread which is considered one-dimensional, while the actual assumed flames for the model are two-dimensional in terms of a planer flame orthogonal to the wall. To be able to use concurrent flame spread simulations to calculate HRR curves, particular attention is given to the overall pyrolysis and burnout areas. Details on pyrolysis and burnout fronts used in the area calculations are provided in Appendix B.

As a simplifying assumption, the pre-heat and spread areas are based on expected burn patterns. In this case, assuming a source fire located directly adjacent to a wall, one might expect vertical flame spread up the wall, fanning out in a semicircular and T-shape manner upon reaching the flat ceiling, if the ceiling material is combustible (see Figure 4 and Appendix B). With this assumption, developing burning area up the vertical wall is relatively straightforward because initially only the source fire width is required. Lateral spread across the wall in the initial growth phase is expected to be comparatively minimal and is neglected during prediction of the initial flame spread. If continued flame spread is predicted, and

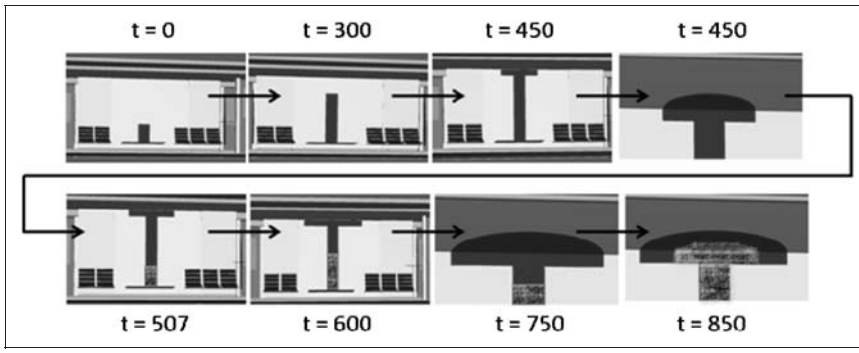

Figure 4. Representative flame spread.

therefore CFD analysis is called for, more complex lateral flame spread can be considered at that stage.

Along the interface of the wall and the ceiling, a region of wall area will experience lateral flame spread. The depth of this region below the ceiling can be estimated as $0.08\,H$, where H is the ceiling height [18].

Based on these assumptions, HRR values are established using pyrolysis areas based on $x_p - x_b$, with the following:

For $X_p < H$ and $X_b < H$

$$\text{HRR vs. Time} = \left(x_p - x_b\right)\left(x_{pow}\right)\left(\dot{E}''\right) \tag{2}$$

For $X_p > H$ and $X_b < H$:

$$\text{HRR vs. Time} = \left[(H - x_b)x_{pow} + 2D\left(x_p - H\right) + \frac{\pi}{2}\left(\frac{x_{pow}}{2} + \left(x_p - H\right)\right)^2\right]\dot{E}'' \tag{3}$$

For $X_p > H$ and $X_b > H$:

$$\text{HRR vs. Time} = \left[2D\left(x_p - x_b\right) + \frac{\pi}{2}\left(\frac{x_{pow}}{2} + \left(x_p - H\right)\right)^2 - \frac{\pi}{2}\left(\frac{x_{pow}}{2} + (x_b - H)\right)^2\right]\dot{E}'' \tag{4}$$

Where, x_{pow} is the initial source fire width, H is the ceiling height and $D = 0.08\,H$ (representative T-shape depth).

With this approach, the source fire is described through definition of the fire geometry height and width, the length of time that the source fire burns (t_{bs}), and the incidental heat flux imposed on the wall. For the sake of simplicity, the length of time that the source fire burns (t_{bs}) is assumed to be equal to the length of time that the initial wall materials burn (t_{bo}).

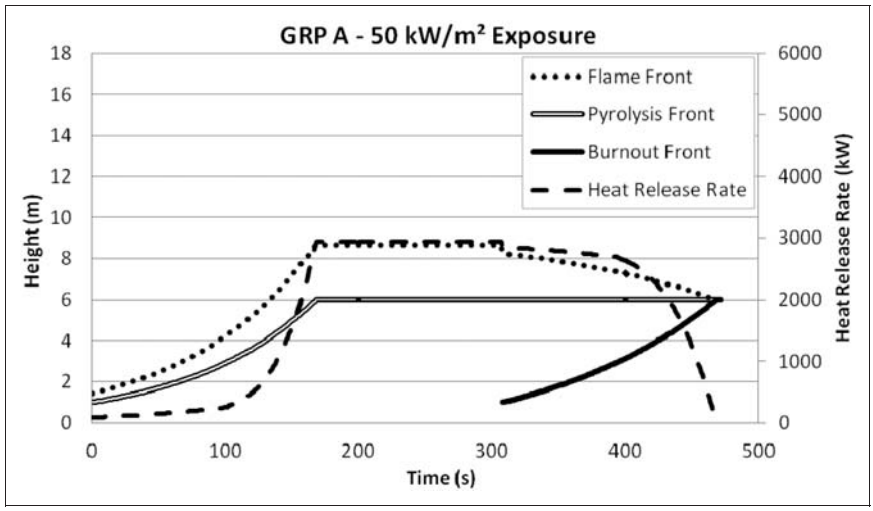

Figure 5. Flame spread analysis results – GRP A with 50 kW/m^2 exposure.
GRP: glass-reinforced polymer.

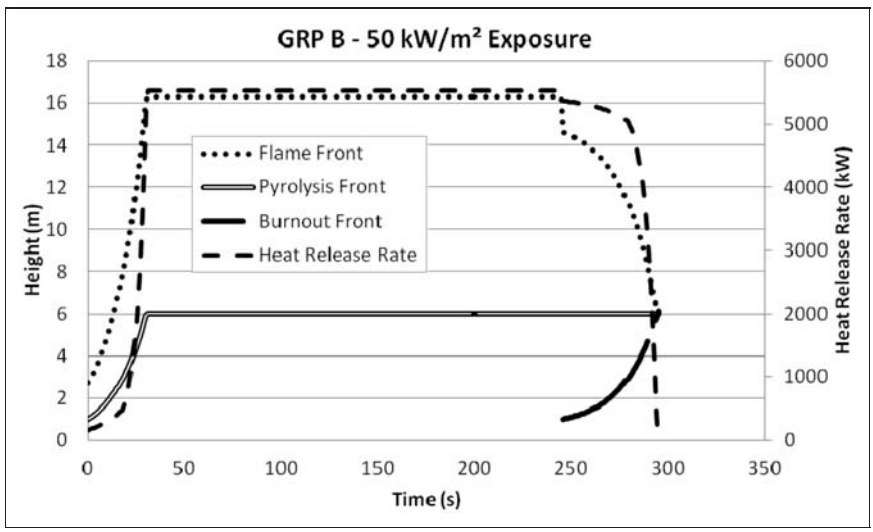

Figure 6. Flame spread analysis results – GRP B with 50 kW/m^2 exposure.
GRP: glass-reinforced polymer.

Appendix B provides example calculations that demonstrate negative and positive b-parameter effects.

Continuing the illustrative example, the above methodology was applied to review initial flame spread behaviors of GRP A and GRP B. Figures 5 and 6

provide example results that show the positions of the flame front, pyrolysis front and burnout front as a function time, as well as the predicted HRR curves for the two GRP materials given an incident heat flux of 50 kW/m^2.

As can be seen in the figures, both materials support flame spread given a heat flux exposure of 50 kW/m^2. However, GRP A exhibits a lower calculated average HRR per unit area than GRP B, and thus the peak HRR for GRP A is lower than that of GRP B. The pyrolysis front for GRP B reaches the ceiling (at 3.0 m) and then the far side of the ceiling (at 6.0 m) more quickly than the pyrolysis front of GRP A does. This indicates that under these conditions, GRP B can be expected to spread flames more rapidly than GRP A. However, the data also suggest that both of these materials are likely to spread flame when subjected to certain levels of heat flux. Therefore, these results are not sufficient to draw conclusions regarding the conformance of these materials to the defined performance criteria and further modeling is required to determine the consequences of this initial flame spread within the rail vehicle.

The modeler must evaluate the precision of this methodology for the specific situation, and must evaluate the impact of the assumptions that are inherent in the approach. Adaptation of this methodology for a specific case will require validation by the modeler.

Integration with CFD

If application of the simplified approach outlined above is not conclusive regarding the potential fire consequences given the vehicle interior materials (e.g. if continued but not rapid flame spread is predicted), CFD analysis may be required in order to develop overall fire hazard conclusions. Also, geometries and arrangements that may be expected to support flame spread (closely spaced combustible seats, combustible materials lining the ceiling, etc.) may require advanced analysis even if the simplified approach indicates that the initial burning material represents a limited flame spread hazard. A large number of possible material and geometrical conditions are possible in the design of passenger rail vehicles; therefore the engineer must consider these factors when evaluating the need for advanced analysis.

An approach using FDS [7] has been developed which includes the following steps:

1. Determine CFD model input parameters needed to simulate various design fires.
2. Simulate various design fires within the vehicle using CFD for each material.
3. Model initial flame spread as a series of burners that together recreate the flame spread behavior predicted by the simplified analysis outlined above.
4. Model combustibility characteristics of adjacent surface materials by distilling material parameters from cone calorimeter data, in this case through application of a GA analysis.
5. Use CFD results to inform the material choice and to help understand the overall fire hazard associated with the vehicle.

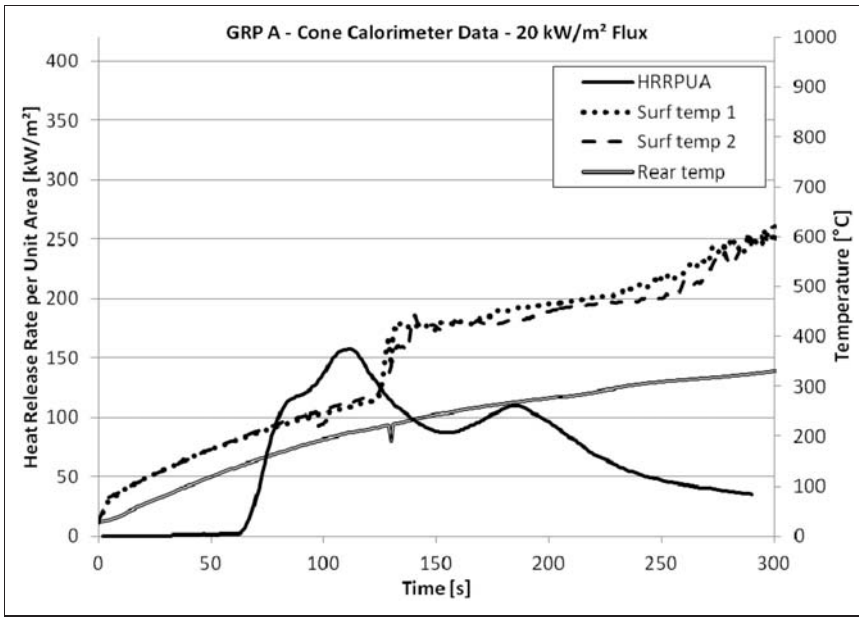

Figure 7. Cone calorimeter data – GRP A with 20 kW/m^2 flux.
GRP: glass-reinforced polymer.

The application of CFD to rail vehicle fire hazard modeling and the use of a GA for estimating FDS parameters is discussed in the literature [19] and will not be expanded upon here. However, FDS has not been validated for flame spread [2]. As such, the unique approach taken here is to manually specify initial ignition and flame spread on the wall materials in the FDS model to match the predictions generated by the simplified flame spread calculation. A series of burner surfaces is implemented in the model; these burners are sized and prescribed with individual HRR curves such that, at any given time, the extent of the pyrolysis area and the total HRR are equivalent to that predicted by the initial flame spread analysis.

To obtain necessary pyrolysis data for the illustrative example materials, cone calorimeter tests were carried out according to ASTM standards [6]. Thermocouples were added to the apparatus to record specimen front and back surface temperatures needed for determining FDS input parameters; temperature data obtained using an infrared camera were not used in developing material properties due to concerns related to the accuracy of the camera in tracking surface temperatures when flames are present. The specimen holder was modified so that temperature measurements could be taken inside the sample (where possible) and on the back face of the sample. GRP A and GRP B were exposed to heat flux levels of 15, 20, 50, and 75 kW/m^2. Figures 7 to 10 show derived average HRRPUA values based on the 20 and 50 kW/m^2 tests.

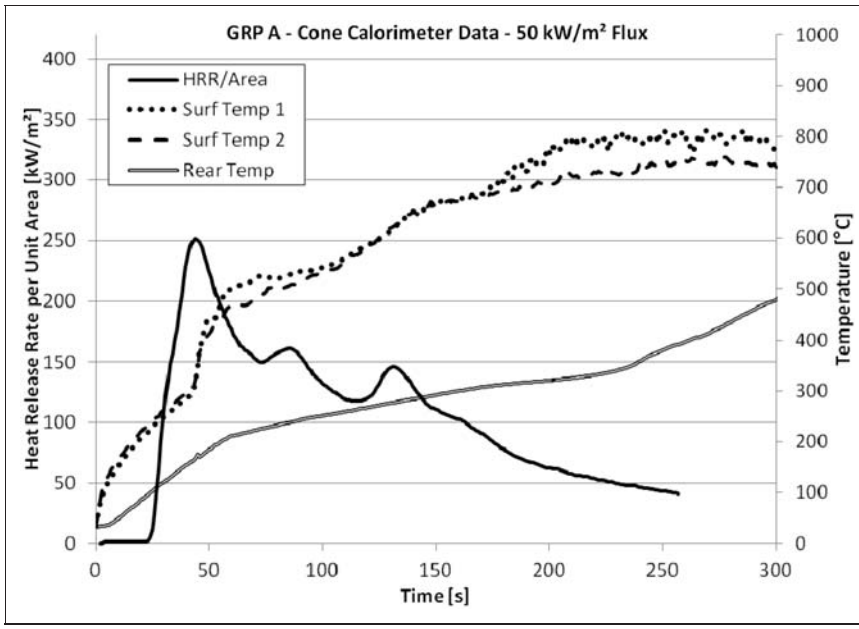

Figure 8. Cone calorimeter data – GRP A with 50 kW/m^2 flux.
GRP: glass-reinforced polymer.

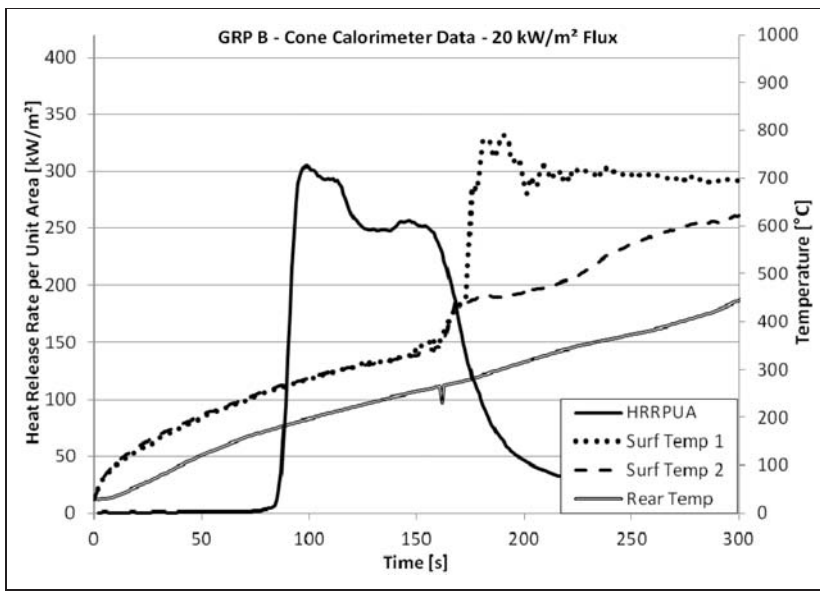

Figure 9. Cone calorimeter data – GRP B with 20 kW/m^2 flux.
GRP: glass-reinforced polymer.

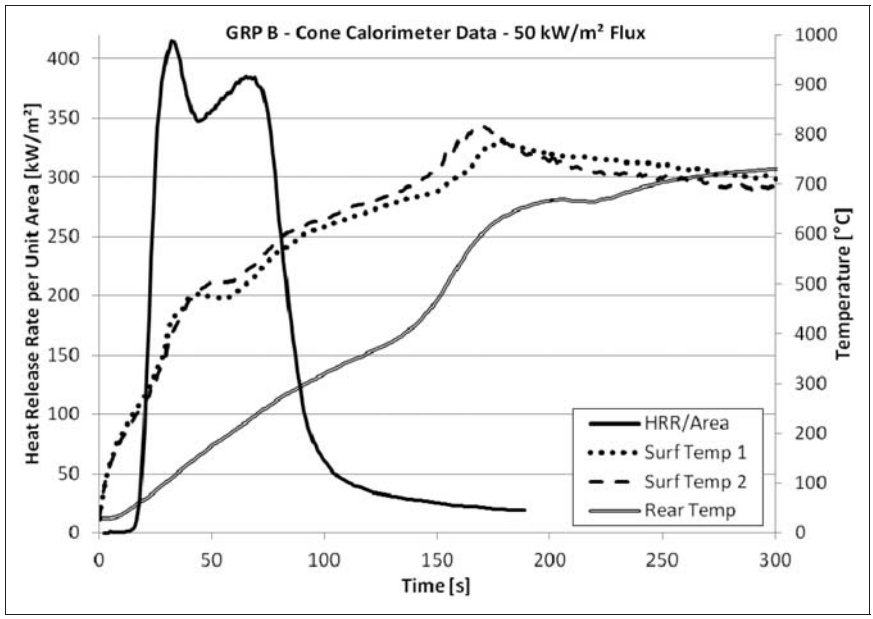

Figure 10. Cone calorimeter data – GRP B with 50 kW/m^2 flux.
GRP: glass-reinforced polymer.

Table 2. GRP surface input parameters

	Input values	
Parameter	GRP A	GRP B
Stretch factor	1.000	1.000
Cell size factor	0.500	0.500
Thickness	0.0027 m	0.0035 m
Back boundary condition	Insulated	Insulated
Shrinking material	False	False
Initial solid temperature	27.0°C	27.0°C

GRP: glass-reinforced polymer.

Several input parameters in FDS are used to describe the composition of solid surfaces [7]. Listed in Tables 2 and 3 are the material parameters determined through use of the GA for the two example materials. Additional material input parameters are discussed in Appendix C. The use of the GA and the derivation of material properties for use in CFD modeling is not the focus of this article, so discussion of the technique is limited here. For greater detail, refer to work by Lautenberger et al. [20].

Table 3. GRP surface input parameters virgin vs. char

	Input values			
	GRP A		GRP B	
Parameter	Virgin	Char	Virgin	Char
Mass fraction	1.000	0.000	1.000	0.000

GRP: glass-reinforced polymer.

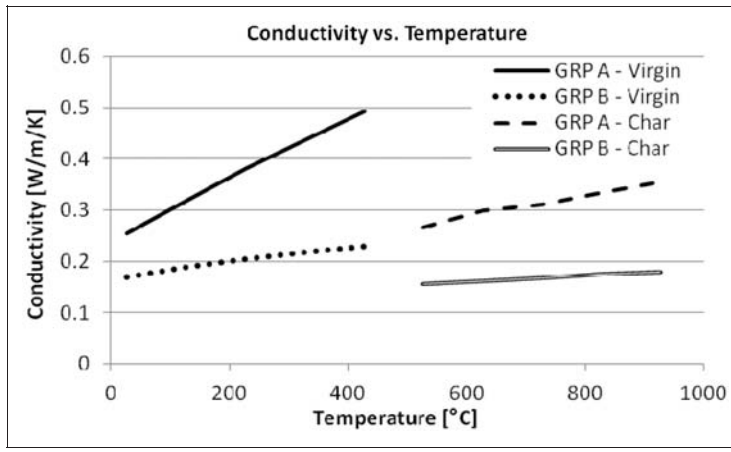

Figure 11. GRP conductivity temperature dependence.
GRP: glass-reinforced polymer.

The parameters *cell size factor* and *stretch factor* allow the user to increase the numerical stability of the pyrolysis calculation. By setting cell size factor to 0.5, the surface mesh cells that are used to calculate heat transfer are reduced in size to half of the size calculated through a default rule in FDS. This rule bases the surface mesh cell size on the square root of the material's thermal diffusivity. Setting the stretch factor to 1.0 forces the surface mesh cells to be uniform in size.

Table 3 represents the initial state of the surface (virgin, unburned GRP), so the state that remains after pyrolysis (char) composes zero percent of the mass of the surface.

The conductivity and specific heat of these materials change with temperature. The graphs in Figures 11 and 12 show the temperature dependence of these parameters as predicted by the GA analysis for the GRP materials.

With the GA-derived input data, an FDS model of an example vehicle was developed to evaluate the impact of the two GRP materials. Within the FDS model, all wall and ceiling surfaces, including door interior linings, were composed

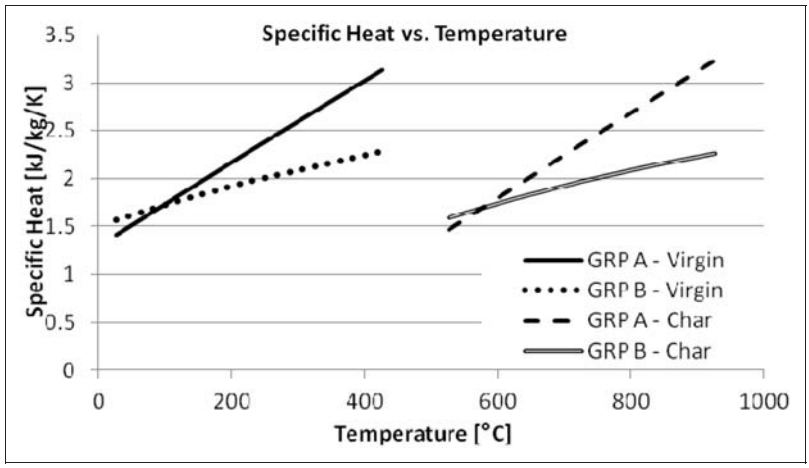

Figure 12. GRP specific heat temperature dependence.
GRP: glass-reinforced polymer.

of the GRP material being considered. Seats were assumed to be comprised of steel structures with plastic sides and backs and carpet-like seat surfaces. The flooring was assumed to be a rubber-based flooring material. This combination of materials is typical of certain types of subway or other short-trip passenger rail vehicles, and has been used here to illustrate the overall approach without introducing a large number of different materials. Other types of rolling stock, such as commuter rail vehicles, may have different combinations of materials that can contribute to fire spread; each material present in a vehicle should be evaluated for its potential to contribute to overall fire growth.

Since the seat and floor materials are not being evaluated here, the different models evaluating GRP A and GRP B assumed the same seat and floor materials. All windows were assumed to be glass. Breakage of windows was not modeled. It was assumed that all doors on one side of the car were open during the modeled fire scenario. This represents a condition where the car is parked at a station with the doors on one side open. End car doors were assumed to be closed. Effects of station geometry and fire protection systems (such as sprinklers and smoke control) were not modeled because the intent of the analysis was to evaluate the effect of different materials on overall fire size. The smoke was assumed to vent from the train to an infinite volume. Based on past research [20], it has been shown that for fire sizes and materials typical of passenger rail vehicles, flame spread is predicted well with a grid resolution of 50 mm, which was used in this case. Listed in Table 4 are the fuel reaction properties used in FDS [7] to represent the GRP materials.

The initial temperature for the ambient environment (inside and outside of the train) and all surface boundaries has been specified as 20°C. The spread of smoke has been calculated using large eddy simulation techniques, in which the large-scale eddies are computed directly and the sub-grid scale dissipative process is

Table 4. GRP reaction properties

Property		Value
Heat of combustion		11,000 kJ/kg
Soot yield		0.096 g_{soot}/g_{fuel}
CO yield		0.058 g_{CO}/g_{fuel}
Chemical reaction	Carbon atoms	2.1
	Hydrogen Atoms	2.0
	Oxygen atoms	1.0

GRP: glass-reinforced polymer.

empirically modeled. This means that the large-scale mixing taking place between the plume/smoke layer and the ambient air is computed directly through first principles by the CFD model. For the purposes of this demonstration, a single initiating fire on the floor of a vehicle directly adjacent to a wall has been considered. An analysis of a proposed rail vehicle should include attention to a range of design fire scenarios.

The materials being considered here have strongly positive b-parameter values when exposed to heat flux values on the order of 50 kW/m^2. In order to cause this level of heat flux, the CFD analysis has assumed that a 500 kW source fire occurs in contact with a wall of the vehicle (a 500 kW fire is representative of several bags of trash).

As discussed previously, initial ignition and flame spread on the wall materials in the FDS model were manually specified using burner surfaces to match the initial flame spread model. Figures 13 and 14 show how the initial HRRs prescribed in FDS align with the curves calculated during the initial flame spread analysis. Additional material ignition beyond the prescribed initial burning area is predicted by FDS using the material properties determined through the GA analysis.

Figure 15 provides a comparison of the total HRR of the passenger rail vehicle given the two types of lining materials being considered. Again, alignment is seen between the HRRs from FDS and that from the flame spread model for initial stages of burning. The HRR is later seen to continue to increase in the FDS simulation as adjacent materials are determined by FDS to ignite.

GRP A results in a peak HRR of approximately 9.2 MW and exhibits a defined decay phase shortly after the peak HRR is experienced. GRP B results in a maximum HRR of approximately 12.0 MW with a sustained HRR of approximately 11.0 MW subsequent to the peak for the remaining simulated duration. Because the maximum HRR was the focus of this analysis, the simulations were not run until complete burn-out. The example analysis provided here illustrates that the installation of GRP A will result in a maximum HRR of less than the stated criterion of 11.0 MW. The other material considered, GRP B, results in a maximum HRR of approximately 12.0 MW, which exceeds the stated limit.

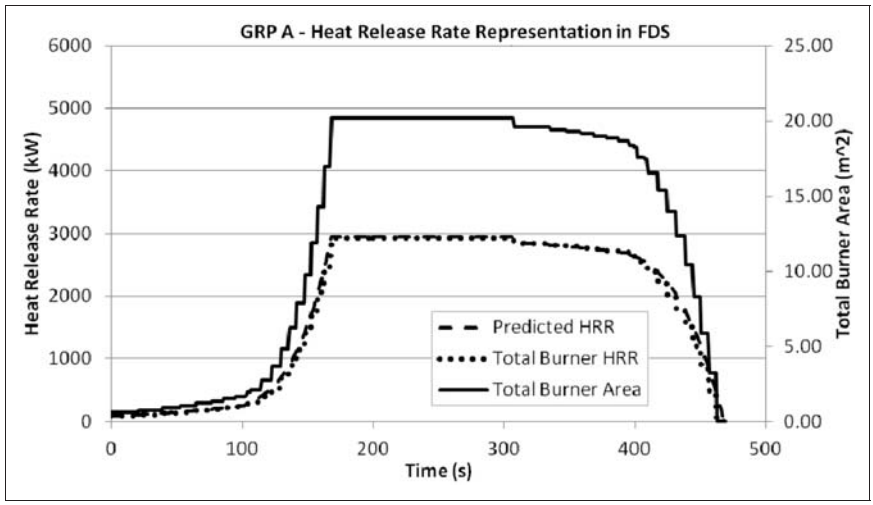

Figure 13. GRP A – heat release rate curve representation in FDS.
GRP: glass-reinforced polymer; FDS: fire dynamics stimulator.

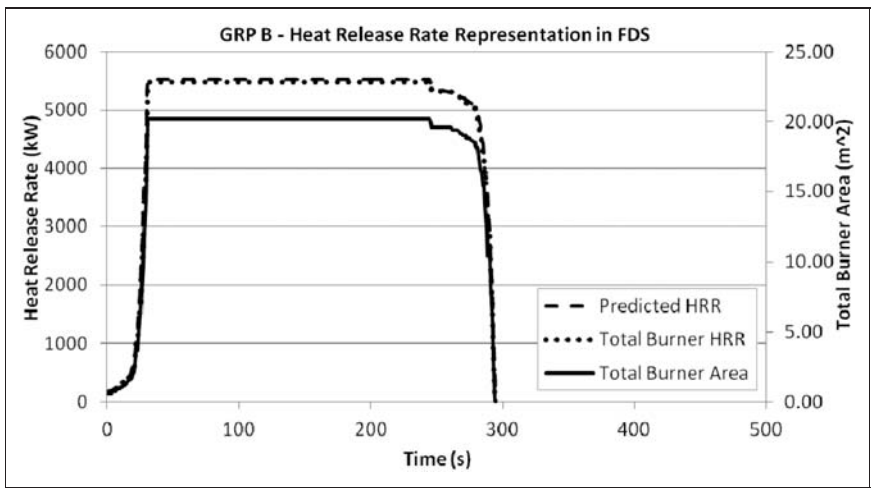

Figure 14. GRP B – heat release rate curve representation in FDS.
GRP: glass-reinforced polymer; FDS: fire dynamics stimulator.

While reviewing this example, it should be cautioned that this analysis has not specifically addressed life safety within the rail vehicle or associated tunnels or stations, nor has it considered the possible impact of additional design initiating fires, vehicle layouts, or ventilation conditions. Each of these factors may need to be considered when carrying out this type of study for an actual project.

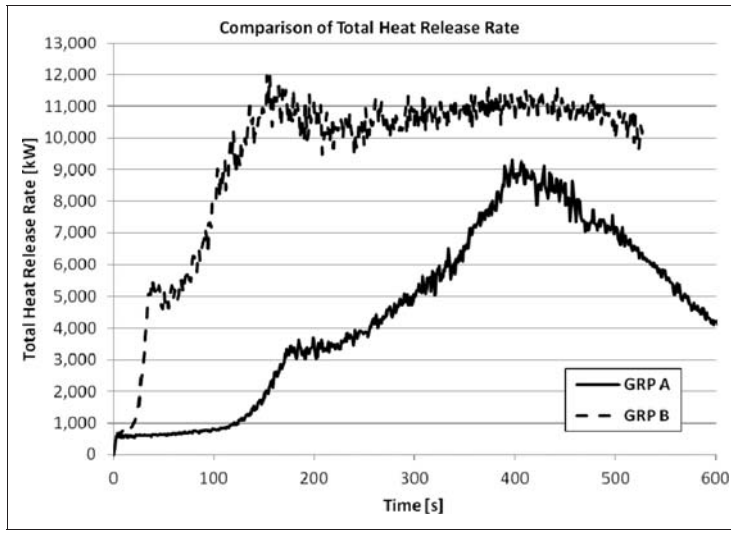

Figure 15. Comparison of total heat release rates from FDS.
FDS: fire dynamics stimulator.

Limitations

This approach uses a combination of small-scale test data and simplified analysis tools (b-parameter calculation and simple flame spread model). Each component has associated uncertainty. At the small-scale test level, differences in materials (from one sample to another), variations in data collection from different test apparatus, and potential errors in reporting may exist. Development of common protocols for testing, apparatus calibration, and data reporting would help reduce uncertainty in the data. Because the simplified analysis techniques (b-parameter and flame spread model) are intended to provide a simple screening approach, some of the complexity associated with factors such as vehicle geometries were ignored (e.g. it was assumed that walls and ceilings were flat with no obstructions). Geometric details were later incorporated with the integration to CFD. Sensitivity analysis could be undertaken to better understand the importance of these issues relative to the level of accuracy needed in the screening approach, and modifications could be made if appropriate.

Summary

An approach has been developed that illustrates how small-scale test data, coupled with a simplified flame spread model, can be used to screen interior finish materials in passenger rail vehicles for their propensity to spread fire given a range of the source fires as part of a fire TVCRA. This yields a simple ‘go/no-go’ screening

approach for assessing material flame spread potential. If the screening tool is inconclusive or indicates that a material is likely to readily spread flame, a more advanced analysis is required. To consider more complex behaviors associated with a growing fire within a vehicle, this article has also demonstrated how initial flame spread can be modeled in the CFD program FDS using a series of burner surfaces that together represent the total HRR and extent of flame spread as a function of time as predicted by the simplified analysis tools.

Disclaimer

The views and conclusions contained in this document are those of the authors and should not be interpreted as necessarily representing the official policies, either expressed or implied, of the US Department of Homeland Security.

Funding

This material is based upon work supported by the Science & Technology Directorate, US Department of Homeland Security under Award Number 2009-ST-108-000013.

Nomenclature

Notation

E = total HRR (kW)
$\dot{E}$ = average HRR (kW)
k = flame length parameter
V = velocity (m/s)
x = length parameter (m)
t = time (s)
H = ceiling height (m)
q = heat flux (kW)
D = representative T-shape depth (m)

Subscripts

b = burnout zone
bo = burnout measured time
bs = source burnout
e = external
end = end measured Time
f = flame zone
ig = ignition
pP = pyrolysis zone
poh = initial source fire height
pow = initial source fire width
pl = pyrolysis height at t_{bo}

Superscripts

$''$ = per unit area (m^{-2})
s = source fire

References

1. Kang K. A smoke model and its application for smoke management in an underground mass transit station. *Fire Safety J* 2007; Vol. 42: 218–231.
2. Miclea PC, Chow WK, Shen-Wen C, et al. *International tunnel fire-safety design practices*. Ottawa: National Research Council Canada, 2007.
3. Jae Seong R, Ryou HS, Park WH, et al. CFD simulation and assessment of life safety in a subway train fire. *Tunnel Underground Space Technol* 2009; Vol. 24: 447–453.
4. National Association of State Fire Marshals (NASFM). *Recommended fire safety practices for rail transit materials selection*. Prepared for the U.S. Department of Transportation, Federal Transit Administration, Office of Safety and Security, 2008.
5. Meacham BJ, Dembsey NA, Schebel K, et al. Rail vehicle fire hazard guidance, Final Report, Developed under DHS Grant 2009-ST-108-000013, Department of Homeland Security, Science and Technology Directorate, International Cooperative Programs Office, Washington, DC, July 2010.
6. ASTM E-1354. Standard test method for heat and visible smoke release rates for materials and products using and oxygen consumption calorimeter. In: *Annual Book of ASTM Standards*. vol. 07.07. West Conshohocken, PA: ASTM International, 1997.
7. McGrattan K, Klein B, Floyd J, et al. *Fire dynamics simulator (version 5) – user's guide*. Gaithersburg, MD: National Institute of Standards and Technology, 2008.
8. Capote JA, Alvear D, Lazaro M, et al. Heat release rate and computer fire modelling vs real-scale fire tests in passenger trains. *Fire Mater* 2008; Vol. 32: 213–229.
9. Cleary T and Quintiere J. *A framework for utilizing fire property tests*. Gaithersburg, MD: National Institute of Standards and Technology, 1991.
10. Cleary T and Quintiere J. A framework for utilizing fire property tests. In: *Fire Safety Science - Proceedings of the Third International Symposium*,1991, Edinburgh, Scotland, pp. 647–656. London: Elsevier Science Publishers Ltd.
11. Meacham BJ, Dembsey NA, Tubbs J, et al. A simplified approach for assessing initial fire development and spread in passenger rail vehicles. *Transport Res Rec* 2011; 2261: 57–63.
12. Meacham, B.J., Dembsey, N.A., Johann, M., et al. Use of small-scale test data to enhance fire-related threat, vulnerability, consequence and risk assessment for passenger rail vehicles. *J Homeland Secur Emerg Manage* 2012; 9: 1–16.
13. Tewarson A. Generation of heat and gaseous, liquid, and solid products in fires. In: DiNenno PJ (ed.) *The SFPE handbook of fire protection engineers*. Quincy, MA: NFPA International, 2008, pp.3:109–3:194.
14. Quintiere JG. A theoretical basis for flammability properties. *Fire Mater* 2005; Vol. 30: 175–214.

15. Dembsey NA and Williamson RB. Coupling the fire behavior of contents and interior finishes for performance fire codes: evaluation of a fire spread model. *J Fire Protec Eng*1997; 8: 119–131.
16. Avila MB. *The effect of resin type and glass content on the fire engineering properties of typical FRP composites*. Worcester, MA: Worcester Polytechnic Institute, 2007.
17. Mowrer FW and Williamson RB. Flame spread evaluation for thin interior finish materials. In: *Fire safety science - proceedings of the third international symposium,* 1991, Edinburgh, Scotland, pp. 689–698. London: Elsevier Science Publishers Ltd.
18. Quintiere J. A simulation model for fire growth on materials subject to a room-corner test. *Fire Safety J* 1993; Vol. 20: 313–339.
19. Kim E. Dembsey N.and Lautenberger C. Parameter estimation for pyrolysis modeling applied to polyester FRP composites with different glass contents. *''Fire and Materials 2009, 11th International Conference and Exhibition''* 2009, San Francisco, CA, pp. 61–76.
20. Lautenberger C, Wong W, Coles A, et al. Large-scale turbulent flame spread modeling with FDS5 on charring and noncharring materials. *''Fire and Materials 2009, 11th International Conference and Exhibition''* 2009, San Francisco, CA, pp. 367–378.
21. Quintiere J, Harkleroad M and Hasemi Y. Wall Flames and Implications for Upward Flame Spread. *Combust Sci Technol* 1986; Vol. 48: 191–222.
22. Saito K, Quintiere J, and Williams F. Upward turbulent flame spread. *Fire Safety Science - Proceedings of the First International Symposium*, 1986, Gaithersburg, MD, pp. 75–86. London: International Association for Fire Safety Science.
23. Beaulieu P and Dembsey N. Effect of oxygen on flame heat flux in horizontal and vertical orientations. *Fire Safety J* 2008; Vol. 43: 410–428.
24. Babrauskas V. Heat release rates. In: *SFPE handbook of fire protection engineering*. 4th ed., section 3, chapter 1, pp. 1–59. Philip Di Nenno, et. al Quincy, MA: National Fire Protection Association, 2008.

Appendix A

b-Parameter data sets

Calculation of the b-parameter for a range of materials can result in a comparison of the relative propensities of these materials to support flame spread. In turn, this information can be used to inform decisions regarding material choices in the context of established performance criteria.

For example, Figure 16 indicates that the sample called GRP Gel Coat will accelerate flame at lower heat fluxes than the sample called plywood ceiling with white laminated front and timber grain back.

Figure 16 to 18 illustrate a variety of representative materials that are representative of those used in passenger rail vehicles.

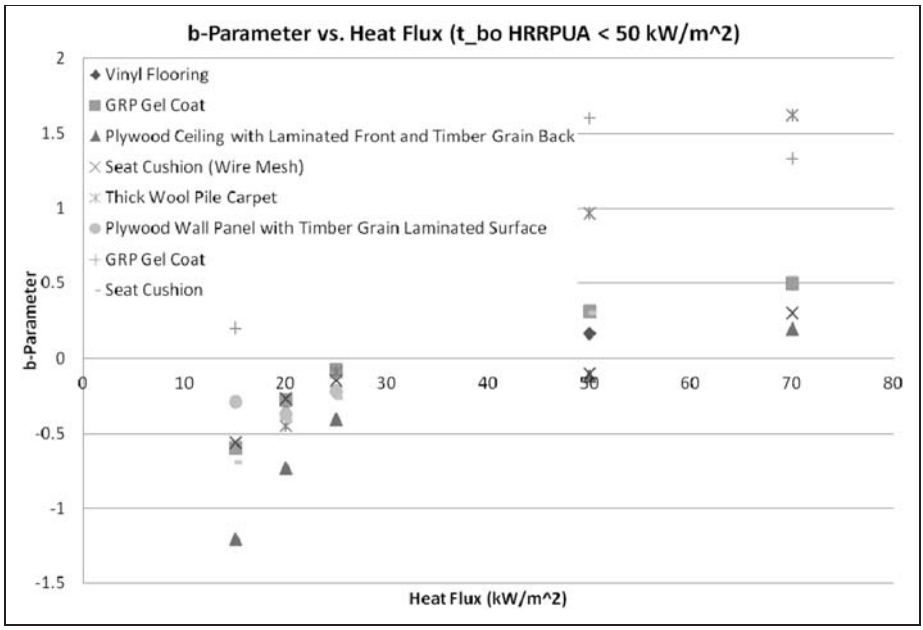

Figure 16. b-Parameter data set 1.

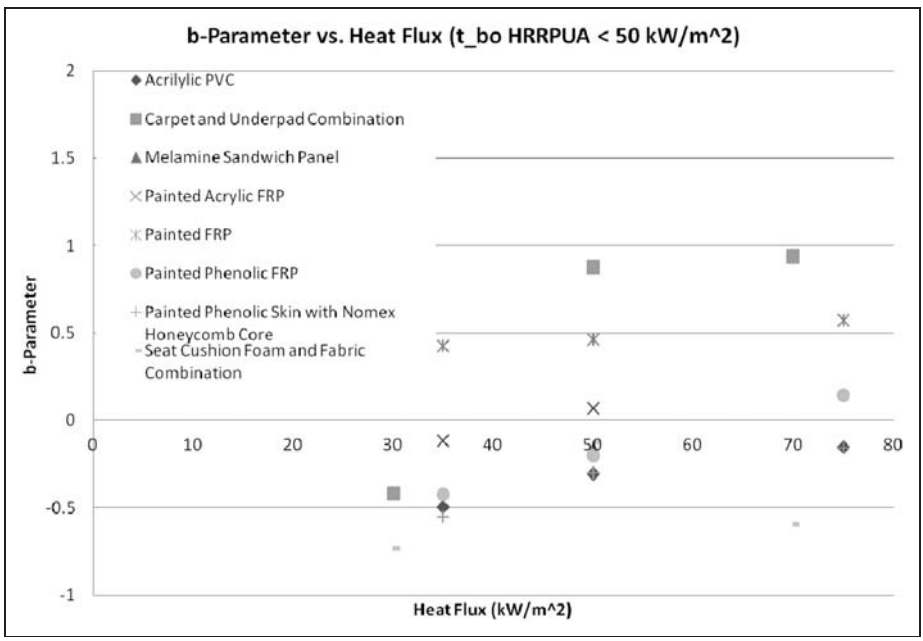

Figure 17. b-Parameter data set 2.

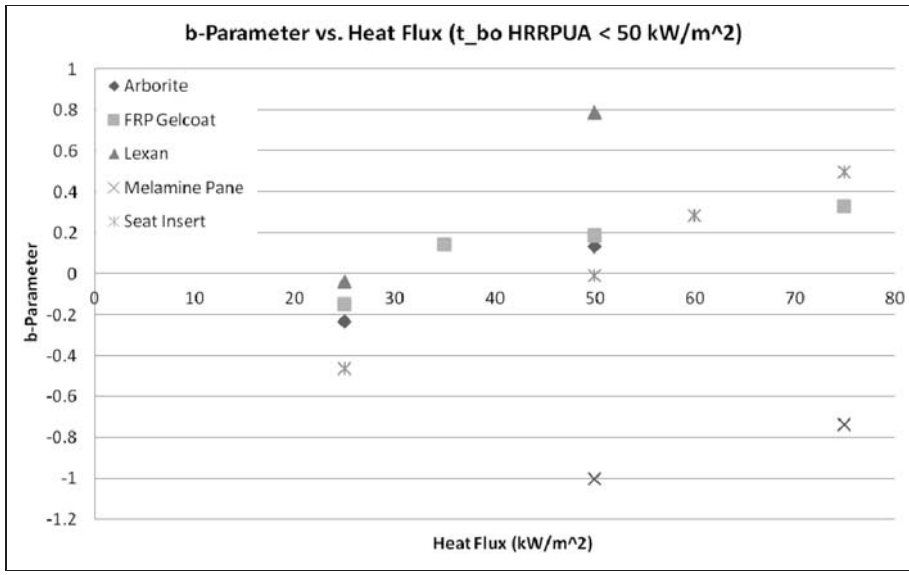

Figure 18. b-Parameter data set 3.

Appendix B

Simplified flame spread model

Mowrer and Williamson [17] show that the flame spread rate is related to the advancement of the pyrolysis front

$$V_p = \frac{x_f(t) - x_p(t)}{t_{ig}} \tag{5}$$

The characteristic flame spread time, t_{ig}, is the time to ignition from each of the cone calorimeter tests [6]. Obtaining t_{ig} directly from cone data further simplifies the model by directly incorporating parameters such as the ignition temperature and thermal inertia. Once burnout initiates, the rate of fuel burnout can be shown from [17] to be as follows

$$V_{bo} = \frac{x_p(t) - x_b(t)}{x_{bo}} \tag{6}$$

From these initial conditions, the model is divided into near field and far field zones. The near field zone is comprised of the source fire with its incident heat flux and geometric configuration. The heat flux represents the time period from the

source ignition, t_{ig}^{s}, to the source burnout time, t_{b}^{s}. The characteristic geometry considers the height and width of the initial source fire, x_{poh} and x_{pow}, respectively. This model assumes that initial wall ignition is based on the source fire.

The far field zone is comprised of the wall flame zone above the source fire. The time to ignition, t_{ig}, based on the forward zone heat flux, is taken directly from the cone calorimeter [6]. The far field zone will also consider $\dot{E}''$ and t_{bo} based on the pyrolysis zone heat flux. The losses from the forward heating zone are not accounted for. The pyrolysis zone heat flux is assumed to be the prescribed cone calorimeter insult heat flux plus an additional 20 kW/m^2, from the flaming sample. For example, if the prescribed heat flux insult in a given cone calorimeter test is 50 kW/m^2, the total assumed pyrolysis zone heat flux is 70 kW/m^2 (50 kW/m^2 + 20 kW/m^2). The prescribed cone calorimeter heat flux represents an external insult, while the additional 20 kW/m^2 accounts for the insult to the material surface from the flames that result from the burning of that material. The engineer should evaluate the appropriateness of this approach for each material being considered.

As a simplified approach, t_{b}^{s} and t_{bo} are considered to be the same value, taken as the burnout time observed in the cone calorimeter. Mowrer and Williamson [17] further integrate their governing equations to develop equations for pyrolysis height, x_p, with the following limitations:

$$x_p : t < t_{bo} : x_p = x_{po} \exp\left[\left(k_f \dot{E}'' - 1\right)\frac{t}{t_f}\right] \tag{7}$$

Limitations: $x = x_{po}$ at $t = 0$ and $x = x_p$ at t

$$t > t_{bo} : x_p = \left(x_{p1} - x_{po}\right) \exp\left[\left(k_f \dot{E}'' - \frac{t_f}{t_{bo}} - 1\right)(t - t_b)/t_f\right] + x_b \tag{8}$$

Limitations: $(x_p - x_b) = (x_{p1} - x_{\mathrm{po}})$ at $t = t_b$ and $(x_p - x_b) = (x_p - x_b)$ at t

$$x_{\mathrm{f}} : t < t_{bo} : x_f = k_f \dot{E}'' x_p \tag{9}$$

Limitations: Representative flame height based upon linearized flame length approximation [9,21,22].

$$t > t_{bo} : x_f = \left(k_f \dot{E}''\right)\left(x_p - x_b\right) + x_b \tag{10}$$

Limitations: Representative flame height based upon normalized flame length.

Where x_{p1} is the pyrolysis height at t_{bo} and k_f is the correlating factor used to define the flame length ahead of the pyrolysis zone [17].

This value depends on the material being studied and must be chosen on a case by case basis. The value of 0.01 m^2/kW was chosen to demonstrate this method as cone tests were conducted consistent with ASTM E 1354 which requires an insulation substrate [10]. If this substrate is not consistent with the end use application of the materials, then cone tests will need to be conducted with a consistent end use substrate.

$E'' =$ The total heat released or energy released during the cone calorimeter test.

$\dot{E}'' =$ The average HRR, for the purposes of this study, measured from the cone calorimeter test.

Combining equation (6) and equation (8) result in

$$\frac{dx_b}{dt} = \left(x_{p1} - x_{po}\right) \exp\left[\left(k_f \dot{E}'' - \frac{t_f}{t_{bo}} - 1\right)\left(t - t_b^s\right)/t_f\right] t_{bo}^{-1} \tag{11}$$

Rearranging equation (11) and combining constants yields

$$\frac{dx_b}{dt} = C_2 \exp\left[C_1\left(t - t_b^s\right)\right] \tag{12}$$

Where,

$$C_1 = \left(k_f \dot{E}'' - \frac{t_f}{t_{bo}} - 1\right) t_f^{-1} \tag{13}$$

$$C_2 = \frac{x_{p1} - x_{po}}{t_{bo}} \tag{14}$$

Integrating equation (12) results in the burnout height at any time

$$x_b = \left(\frac{C_2}{C_1}\right)\left(\exp\left[C_1\left(t - t_b^s\right)\right] - 1\right) + x_{po} \tag{15}$$

When V_b is larger than V_p (i.e. the burnout front, x_b, is increasing at a greater rate than the pyrolysis front (x_p), the pyrolysis length is decreasing and the material is approaching burnout.

As a proof of concept and to illustrate the effects of negative and positive b-parameter values, both small and large representative source fire scenarios were analyzed. The analysis considered an example FRP gelcoat material under different levels of external incident heat flux. Incident heat flux levels of 25 and 50 kW/m^2 were chosen to represent a range of sizes of initial fires occurring

Table 5. Cone calorimeter results for fiber-reinforced polymer gel coat

Scenario	Heat flux (kW/m^2)	t_{ig} (s)	E'' (kJ/m^2)	$\dot{E}''$ (kW/m^2)	t_{bs} (s)	b-Parameter
Small fire	25	447	49,919	141	801	−0.148
Large fire	50	246	43,604	167	507	0.185

in proximity to the material being considered. This range was chosen based on the work by Beaulieu and Dembsey [23] where inward total heat flux levels were compared to flame heights for wall fires. Given a fire located against a wall, an inward total heat flux of 25 kW/m^2 is representative of a flame height of approximately 0.5 m, while an inward total heat flux of 50 kW/m^2 is representative of a flame height of approximately 1 m. These heat flux values were assumed for source fires located directly adjacent to a wall or for wall fire flame spread.

Given an incident heat flux of 25 kW/m^2 in the cone calorimeter, a b-parameter value of −0.15 was calculated. When the same material was exposed to an incident heat flux of 50 kW/m^2, the resulting b-parameter was calculated to be 0.19. Cone calorimeter results for the 25 kWm^2 and the 50 kW/m^2 fire scenarios can be seen in Table 5. The small source fire scenario is representative of a waste paper basket with an HRR of approximately 40 kW [24] that is assumed to be located directly adjacent to a wall. It is reasonable to use this source fire scenario in the context of rail vehicles because waste paper baskets tend to contain crumpled up paper, debris and other miscellaneous trash that may be involved in an intentional or accidental fire in a passenger rail vehicle. The wall area exposed to the fire's incident heat flux (25 kW/m^2) was assumed to be 0.5 m tall by 0.3 m wide.

The larger source fire scenario is representative of 0.5 L of gasoline on vinyl flooring with an HRR of approximately 500 kW [24]. This scenario is representative of an intentional scenario involving a flammable liquid. The fire in this case was assumed to be 1.0 m tall × 0.6 m wide. With an HRR of approximated 500 kW, the incident heat flux to the wall was ∼50 kW/m^2 and was applied to a wall area ∼1.0 m tall × 0.6 m wide.

Appendix C

GRP material input parameters

Table 6 represents additional material input parameters determined through the use of the GA analysis for GRP A and GRP B:

Table 6. GRP material input parameters

	Input values	
Parameter	GRP A virgin	GRP B virgin
Density	1721.0 kg/m^3	1312.6 kg/m^3
Emissivity	0.864	0.867
Conductivity	See Figure 11	See Figure 11
Specific heat	See Figure 12 (kJ/(kg K))	See Figure 12
Absorption coefficient	0.10E + 7/m	0.10E + 7/m
Residue	GRP_A_char	GRP_B_char
Pre-exponential factor (*A*)	0.74E + 9	0.23E + 10
Activation energy (*E*)	0.12E + 6 kJ/kmol	0.13E + 6 kJ/kmol
Exponent of mass fraction	1.210/s	1.500/s
Heat of reaction	1636.1 kJ/kg	682.8 kJ/kg
Fuel yield	0.400 kg/kg	0.544 kg/kg
Residue yield	0.600 kg/kg	0.456 kg/kg
Steam yield	0.000 kg/kg	0.000 kg/kg
Number of reactions	1	1
Parameter	GRP A Char	GRP B Char
Density	1032.6 kg/m^3	598.9 kg/m^3
Emissivity	0.927	0.924
Conductivity	See Figure 11	See Figure 11
Specific heat	See Figure 12	See Figure 12
Absorption coefficient	0.10E + 7/m	0.10E + 7/m
Number of reactions	0	0

GRP: glass-reinforced polymer.